Role of Proteins of the Ena/VASP Family in Actin-based Motility of *Listeria monocytogenes*

Valérie Laurent,* Thomas P. Loisel,* Birgit Harbeck,‡ Ann Wehman,§ Lothar Gröbe,‖ Brigitte M. Jockusch,‡ Jürgen Wehland,‖ Frank B. Gertler,§ and Marie-France Carlier*

*Dynamique du Cytosquelette, Laboratoire d'Enzymologie et Biochimie Structurales, CNRS, 91198 Gif-sur-Yvette, France; §Department of Biology, Massachusetts Institute of Technology, Cambridge, Massachusetts 02139; ‡Cell Biology, Zoological Institute, Technical University, 38092 Braunschweig, Germany; and ‖National Research Center for Biotechnology, 38124 Braunschweig, Germany

Abstract. Intracellular propulsion of *Listeria monocytogenes* is the best understood form of motility dependent on actin polymerization. We have used in vitro motility assays of *Listeria* in platelet and brain extracts to elucidate the function of the focal adhesion proteins of the Ena (*Drosophila* Enabled)/VASP (vasodilator-stimulated phosphoprotein) family in actin-based motility. Immunodepletion of VASP from platelet extracts and of Evl (Ena/VASP-like protein) from brain extracts of Mena knockout (−/−) mice combined with add-back of recombinant (bacterial or eukaryotic) VASP and Evl show that VASP, Mena, and Evl play interchangeable roles and are required to transform actin polymerization into active movement and propulsive force. The EVH1 (Ena/VASP homology 1) domain of VASP is in slow association–dissociation equilibrium high-affinity binding to the zyxin-homologous, proline-rich region of ActA. VASP also interacts with F-actin via its COOH-terminal EVH2 domain. Hence VASP/Ena/Evl link the bacterium to the actin tail, which is required for movement. The affinity of VASP for F-actin is controlled by phosphorylation of serine 157 by cAMP-dependent protein kinase. Phospho-VASP binds with high affinity (0.5×10^8 M^{-1}); dephospho-VASP binds 40-fold less tightly. We propose a molecular ratchet model for insertional polymerization of actin, within which frequent attachment–detachment of VASP to F-actin allows its sliding along the growing filament.

Key words: actin polymerization • *Listeria monocytogenes* • Ena/VASP/Mena • motility • platelet

The intracellular pathogenic bacterium *Listeria monocytogenes* can propel itself in the host cytoplasm. The propulsive force is thought to be generated by the polymerization of actin filaments (Tilney and Portnoy, 1989; Dabiri et al., 1990; Tilney et al., 1990; Sanger et al., 1992; Theriot et al., 1992), in a process mechanistically similar to the actin-based protrusion of the lamellipodium of locomoting cells (for review see Tilney and Tilney, 1993). The assembled filaments are organized in a meshwork or "tail" used by the bacterium as a support for propulsion. The successful in vitro reconstitution of *Listeria* movement in *Xenopus* egg (Theriot et al., 1994; Marchand et al., 1995) or platelet (Carlier et al., 1997; Welch et al., 1997) extracts makes this bacterium a good experimental model for the biochemical and physical approach of the cellular factors responsible for actin assembly at the leading edge of motile cells.

Address correspondence to M.-F. Carlier, LEBS, CNRS, 91198 Gif-sur-Yvette, France. Tel.: (33) 1-69-82-34-65. Fax: (33) 1-69-82-31-29. E-mail: carlier@lebs.cnrs-gif.fr

In recent years, a combination of physical, genetic, and biochemical approaches have led to the view that *Listeria* movement is driven by the turnover of actin filaments (Carlier et al., 1997; Rosenblatt et al., 1997). The growth of barbed ends, restricted to the bacterium surface and initiated by the bacterial protein ActA (Domann et al., 1992; Kocks et al., 1992), is fed by the pointed end depolymerization of filaments in the medium, including the ones that form the actin tail attached to the bacterium. Hence, during steady locomotion, the length of the actin tail is maintained constant. A Brownian ratchet mechanism (Mogilner and Oster, 1996) has been proposed as a model for actin-based motility of *Listeria*, within which structural fluctuations of the actin meshwork allow insertional polymerization of actin to push the bacterium in the direction of growth of this meshwork.

The above description of *Listeria* movement implies that many cell components are needed to generate motility. Proteins regulating actin dynamics such as capping proteins, ADF/cofilin, and profilin play an important role in enhancing filament turnover, i.e., in increasing the site-

© The Rockefeller University Press, 0021-9525/99/03/1245/14 $2.00

directed barbed end growth (Carlier, 1998; for review see Didry et al., 1998). Proteins that cross-link actin filaments such as alpha-actinin (Dold et al., 1994) organize the actin tail in a rigid meshwork allowing the generation of force. Recent reports have shown that a multiprotein complex, isolated from platelet extracts, containing the actin-related proteins Arp2 and Arp3, is sufficient to initiate actin polymerization at the surface of *Listeria* (Welch et al., 1997), most likely by interacting with ActA (Welch et al., 1998). The Arp2/3 complex remains bound to the pointed ends of nucleated filaments and is uniformly distributed throughout the actin tail while the bacterium is moving (Welch et al., 1997). The existence of a critical concentration for Arp2/3-capped pointed ends (Mullins et al., 1998) indicates that monomer–polymer exchanges occur at the capped ends. This is consistent with pointed end depolymerization in the tail and a filament half-life of ~1 min (Theriot et al., 1992), except perhaps in the axial core of long filaments forming protrusions (Sechi et al., 1997). Strikingly, the actin meshwork assembled at the surface of *Listeria* by Arp2/3 alone is unable to generate propulsion of the bacterium. Therefore, crucial issues remain to be solved to understand the molecular mechanism by which the filaments are nucleated and remain attached while growing at the bacterium surface, and how the spatial organization of the actin meshwork is achieved, as the filaments grow, to produce force and movement. The targets of the *Listeria* protein ActA clearly must play a role in establishing a dynamic link between polymerizing filaments and the bacterium surface. Genetic studies have shown that the 639–amino acid ActA protein, which is anchored by its COOH-terminal region, to the bacterial membrane, possesses two regions important for motility. The NH_2-terminal region (1–262) appears solely responsible for actin nucleation (Pistor et al., 1995; Lasa et al., 1997). The central domain (263–390), which contains four proline-rich repeats, also found in the cytoskeletal proteins vinculin and zyxin (Reinhard et al., 1995), controls the rate of movement (Pistor et al., 1995; Smith et al., 1996; Lasa et al., 1997; Niebuhr et al., 1997). The proline-rich repeats of ActA form the binding site for vasodilator-stimulated phosphoprotein (VASP)[1] or Mena, the only host proteins thus far known to bind to ActA and to remain localized to the bacterium–actin interface as *Listeria* is moving (Chakraborty et al., 1995; Gertler et al., 1996).

VASP and Mena belong to the Ena-VASP family of proteins (Gertler et al., 1996) which share homology with the *Drosophila* Enabled (Ena) protein, known to be involved in neural development (Gertler et al., 1990, 1995). These proteins localize at focal contacts and in regions where actin filaments are highly dynamic (Gertler et al., 1996). They are organized in three domains, an EVH1 (Ena-VASP-homology 1) NH_2-terminal domain, a proline-rich central domain, and an EVH2 COOH-terminal domain. The EVH1 domain mediates the interaction of VASP (Gertler et al., 1996; Niebuhr et al., 1997) and of Mena, the murine homologue of Ena (Gertler et al., 1996), with the proline-rich repeats of ActA. In mammalian cells, proteins of the Ena/VASP family are thought to be targeted to focal adhesions due to the interaction of their EVH1 domain with the ActA-homologous proline-rich motifs of zyxin (Reinhard et al., 1995; Gertler et al., 1996), and may also similarly interact with vinculin (Brindle et al., 1996; Gertler et al., 1996; Reinhard et al., 1996; Hüttelmaier et al., 1998). VASP has also been shown to bind F-actin (Reinhard et al., 1992). Ena/VASP proteins possess a proline-rich region, comprising a $(GP_5)_3$ sequence (Haffner et al., 1995; Gertler et al., 1996) present as a single or repeated motif in the different proteins. Profilin binds VASP and Mena in vitro (Reinhard et al., 1995; Gertler et al., 1996) and in cell extracts (Lambrechts et al., 1997) probably via the $(GP_5)_3$ repeats (Reinhard et al., 1995; Kang et al., 1997). Profilin actually binds the isolated $(GP_5)_3$ peptide (Domke et al., 1997; Lambrechts et al., 1997), consistent with its ability to bind to poly-L-proline.

The present work focuses on the role of VASP, Mena, and Ena/VASP-like (Evl) proteins in the motility of *Listeria* in platelet and brain extracts. Platelets are rich in actin-binding proteins involved in motility and contain micromolar amounts of VASP, whose phosphorylation by cAMP- and cGMP-dependent kinases correlates with the inhibition of platelet aggregation (Waldmann et al., 1987; Aszodi et al., 1999), hence they represent a choice material for the analysis of the mechanism of site-directed actin assembly in response to signaling. Brain extracts are rich in the Mena and Evl proteins. Motility assays have been performed using immunodepleted and reconstituted platelet extracts and brain extracts from wild-type and Mena knockout (−/−) mice, and combined with the use of peptide mimetics and with in vitro polymerization assays to explore the function of VASP, Mena, and Evl in actin-based motility of *Listeria*.

Materials and Methods

Proteins and Antibodies

Actin was purified from rabbit muscle (Spudich and Watt, 1971) and isolated as Ca-ATP-G-actin by Sephadex G-200 chromatography (MacLean-Fletcher and Pollard, 1980) in G buffer (5 mM Tris-Cl^-, pH 7.8, 0.1 mM $CaCl_2$, 0.2 mM ATP, 1 mM DTT, 0.01% NaN_3). Actin was pyrenyl-labeled (Kouyama and Mihashi, 1981) or rhodamine-labeled on lysines in the F form as described (Isambert et al., 1995). Profilin was purified from bovine spleen as described (Pantaloni and Carlier, 1993).

VASP bacterial recombinant protein was expressed and purified as described (Hüttelmaier et al., 1998).

For recombinant Evl protein, a fragment encoding amino acids 1–393 of Evl was generated via PCR and cloned in pFB-Nhis (GIBCO-BRL). Recombinant protein was obtained and purified using the Bac-to-Bac™ baculovirus expression system (GIBCO-BRL) according to the manufacturer's instructions. Recombinant baculovirus-infected high-five insect cells were harvested and the recombinant protein purified by affinity to Talon resin (Clontech) according to the manufacturer's instructions. The coding region of Evl was amplified for a cDNA using the following primers: forward primer: 5′-Cgg gAT CCA TgA gTg AAC AgA gTA TCT gC-3′, reverse primer: 5′-Cgg Cgg CCg CCg Tgg TgC TgA TCC CAC-3′.

GST fusion proteins of EVH1 domains of Mena or Evl have been described elsewhere (Gertler et al., 1996; Niebuhr et al., 1997). Fragments encoding the EVH1 domain of VASP (amino acids 1–149) or the proline-rich repeat region of ActA (amino acids 241–423) were generated by PCR, and cloned into the pGEX2TK vector (Pharmacia). Prokaryotic recombinant GST-EVH2 (amino acids 226–380) was obtained by generating the fragment from full-length VASP by PCR and cloning it into the pGEX4T1 vector (Pharmacia). The GST fusion proteins were expressed and purified following manufacturer's instructions.

1. *Abbreviations used in this paper:* Ena, *Drosophila* Enabled protein; VASP, vasodilator-stimulated phosphoprotein.

The monoclonal VASP antibody (clone IE245) used in this study was described recently (Abel et al., 1996). The mAb against Evl (clone 84H1) was raised against the GST fusion protein of Evl-EVH1, and specificity was confirmed on pure Evl-EVH1 protein after thrombin digestion of the GST fusion protein. Both antibodies are IgGs and have been purified by affinity chromatography using protein G–Sepharose. The VASP polyclonal antibody M4 was purchased from Immunoglobe.

The $(GP_5)_3$ peptide of the VASP proline-rich region was synthesized with an AMS 222 Multiple Sequencer using TentaGel S resin (Rapp Polymere).

The creation and analysis of the Mena knockout mice is described in Lanier et al. (1999).

Recombinant VASP Protein Construction and Expression in Insect Cells

The complete human VASP cDNA was PCR amplified from a clone (I.M.A.G.E clone 824217) obtained at Genome System Inc., using the following two oligonucleotide primers: 5′-GCG ATA AGG ATC CGa tga gcg aga cgg tca tct g-3′ and 5′-GCG CCT GGT ACC tca ggg aga acc ccg ctt cc-3′. The pBlueBacHis2B-VASP plasmid was generated by ligating the BamH1/Kpn1 double digest PCR fragment with the BamH1/Kpn1 digested pBlueBacHis2 B (Invitrogen BV). The resulting polyhistidine-enterokinase site NH_2-terminal–tagged VASP nucleotide sequence was verified by DNA sequencing.

Generation of the VASP recombinant baculovirus was achieved by using the standard procedure of transfection–recombination in Sf21 insect cells (O'Reilly et al., 1992). Positive virus clones were identified by Western blot analysis using both the M4 anti-VASP rabbit pAb or the anti-Xpress™ mAb (Invitrogen BV).

Sf21 insect cells were cultured in Grace's supplemented media (GIBCO-BRL) containing 10% FBS (GIBCO-BRL) and 0.001% pluronic acid (GIBCO-BRL) in 1 liter polycarbonate Erlenmeyer flask at 27°C under vigorous shaking. 250 ml of cell suspension ($1.5–2.5 \times 10^6$/ml) was infected with the recombinant VASP baculovirus at a multiplicity of infection ranging from 2 to 5 for 60 h.

Purification of Recombinant VASP from Sf21 Insect Cells

Harvested infected Sf21 cells were rinsed once in ice-cold PBS and disrupted on ice in 10 ml of lysis buffer (20 mM sodium phosphate, pH 8.0, 5% glycerol, and 1 mM DTT) containing protease inhibitors (0.5 mM PMSF, 10 μg/ml benzamidine, 5 μg/ml chymostatin, and 5 μg/ml leupeptin). The mixture was centrifuged for 20 min at 45,000 *g* at 4°C. The supernatant was kept on ice. The pellet was resuspended in 10 ml of buffer A (20 mM sodium phosphate, pH 8.0, 300 mM NaCl, 5% glycerol, 0.03% Tween 20, 1 mM DTT, and protease inhibitors), homogenized in a Dounce potter, and left on ice for 30 min before a 20-min centrifugation run at 45,000 *g* at 4°C. The supernatant was added to the first one and the whole solution was dialyzed against 500 ml of 20 mM sodium phosphate, pH 8.0, 5% glycerol, 0.03% Tween 20, and 1 mM DTT (two changes). The cellular extract containing VASP was rapidly drop-frozen in liquid nitrogen and kept at −80°C.

Purification of the insect recombinant VASP was achieved at 4°C by a two-step chromatography procedure. The cellular extract was laid on a 10-ml DEAE-cellulose matrix DE52 (Whatman) equilibrated with buffer B (20 mM sodium phosphate, pH 8.0, 0.5 mM DTT, 5% glycerol, and 0.03% Tween 20) and the protein flow-through was collected. NaCl was added to this protein fraction up to a 50 mM final concentration before mixing with 500 μl of TALON™ metal affinity resin (Clontech) equilibrated with buffer C (20 mM sodium phosphate, pH 8.0, 50 mM NaCl, 5% glycerol, and 0.5 mM DTT) for 30 min. The suspension was deposited on an empty column and the flow-through was discarded. The resin was rinsed with 20 ml of buffer C and VASP was eluted with buffer D (20 mM sodium phosphate, pH 7.0, 50 mM NaCl, 0.5 mM DTT, 5% glycerol, 100 mM imidazole, pH 7.0, 100 mM EDTA, pH 7.0, and protease inhibitors). VASP was dialyzed against VASP buffer (20 mM Hepes-NaOH, pH 7.8, 30 mM NaCl, 1 mM DTT, and 5% glycerol). The composition of VASP buffer was worked out to optimize the solubility of VASP. After centrifugation at 400,000 *g* at 4°C for 30 min, the protein was stored at −80°C at a concentration of 10–20 μM. The concentration of VASP was determined by the Bradford protein assay (Bio-Rad) using BSA as a standard. 2–3 mg of pure VASP was thus obtained from a 250-ml culture. Electrophoretic patterns of the eukaryotic recombinant protein showed two bands migrating as 54- and 50-kD polypeptides, representing 40 and 60% of the material, respectively. Both polypeptides were recognized by the anti-VASP M4 antibody and the anti-Xpress mAb (Invitrogen). After treatment with PKA catalytic subunit, the material migrated as a single 54-kD polypeptide, and after treatment with alkaline phosphatase, as 50 kD. Therefore, the two bands of the eukaryotic recombinant VASP represent the serine 157–phosphorylated VASP (49.5 kD) and the unphosphorylated VASP (46 kD) usually found in platelets (Butt et al., 1994), to which the 4-kD fusion peptide has been added.

Extracts

Platelet extracts were prepared from outdated unstimulated human platelets essentially as described (Laurent and Carlier, 1998). The platelet lysate obtained by sonication in buffer A containing 10 mM Tris-Cl^-, pH 7.5, 10 mM EGTA, 2 mM $MgCl_2$, and antiproteases (10 μg/ml of leupeptin, pepstatin, and chymostatin, and 1 mM PMSF) was centrifuged at 100,000 *g* for 45 min at 4°C. The supernatant was supplemented with 2 mM ATP, 2 mM DTT, and 150 mM sucrose, rapidly frozen on liquid nitrogen, and stored at –80°C.

Mouse brain extracts were prepared by homogenization of brains from freshly decapitated mice in two volumes of ice-cold buffer A, using a 0.5 ml glass/Teflon potter (20 strokes), followed by sonication (3 × 15 s, low power) and centrifugation at 100,000 *g* for 1 h at 4°C. The supernatant was frozen on liquid nitrogen and stored at −80°C.

Bacterial Strains

L. monocytogenes strain Lut12 (pactA3) overexpressing ActA (Kocks et al., 1992; Marchand et al., 1995) was used. Bacteria were grown overnight at 37°C in brain/heart infusion medium in the presence of 7 μg/ml chloramphenicol and 5 μg/ml erythromycin. The culture was then brought into fresh medium (5 ml) at an optical density of 0.3 at 560 nm, and grown to stationary phase (1.5–2.0 OD units at 560 nm). After addition of 30% glycerol to the medium, bacteria were frozen in 100-μl aliquots on liquid nitrogen and stored at −80°C.

In Vitro Motility Assays of Listeria

Frozen bacteria were thawed, centrifuged, and resuspended at 6×10^9 bacteria/ml in B buffer (10 mM Hepes, pH 7.7, 0.1 M KCl, 1 mM $MgCl_2$, 0.1 mM $CaCl_2$, and 50 mM sucrose). The motility assay solution (16 μl) was prepared at room temperature by mixing 4 μl of cytoplasmic brain or platelet extract and 12 μl additional ingredients (from concentrated stock solutions) coming up to the following final concentrations: 0.38% methylcellulose, 5 μM F-actin (added to platelet extracts only), 6 mM DTT, 2 mM ATP, 4 mM $MgCl_2$, 1.5×10^{-3} % DABCO as an oxygen scavenger, 1 μM rhodamine-actin, and 2×10^8 bacteria/ml. After thorough mixing, 2.5 μl of the suspension was squashed between a BSA-coated slide and a 20 × 20-mm coverslip. The depth of the chamber was 6 μm. The sample was sealed with VALAP (Vaseline/lanosterol/paraffin, 1:1:1). Movement of *L. monocytogenes* was observed at room temperature 10 min after preparation of the sample in a Zeiss III RS microscope equipped with a Lhesa LHL4036 silicon-intensified camera. Bacteria were observed both in phase-contrast and in fluorescence. Movement was recorded in real time or time lapse using a Panasonic video recorder. Rates of movement were measured using a Hamamatsu image analyzer. 6–15 measurements were made on different bacteria for each sample. Average rates were derived from the distances moved over a period of 1 min. Standard deviations were calculated using the statistical tools of Kaleidagraph software. Many bacteria (>200) were counted to derive the percentage of motile bacteria in a given experiment. All results shown have been obtained reproducibly in at least four independent experiments, and data shown in figures are typical data.

VASP, Evl, and Profilin Depletion in Platelet or Brain Extracts

VASP was immunodepleted from platelet extracts using 4.5-μm-diameter goat anti–mouse IgG-coated magnetic Dynabeads (Dynal). The binding capacity was 0.3–0.4 μg antibodies per 10^7 beads. 2×10^8 Dynabeads were suspended and extensively washed in PBS containing 1 mg/ml BSA, then incubated with a sixfold excess of monoclonal anti-VASP antibody (mAb 245) which was shown, by epitope mapping, to recognize the proline-rich central region of VASP. The concentration of the antibody was 5.8 mg/ml.

Incubation was carried out for 30 min at room temperature, with rotary stirring. After extensive washing of the beads with PBS containing 0.1% BSA, the beads were split in two batches for two consecutive cycles of depletion. In the first cycle 10^8 anti-VASP–coated beads were incubated with 20 μl of platelet extract at 4°C for 90 min with rotary stirring. The supernatant from the first cycle of depletion was submitted to a second cycle using the second batch of Dynabeads. Mock-depleted extracts were obtained by identical treatment of extracts by uncoated Dynabeads. The extent of VASP deletion was quantitated by immunoblotting using a polyclonal anti-VASP antibody.

Evl immunodepletion from mouse brain extracts was performed as follows. 4×10^8 Dynabeads were coated (to saturation) with monoclonal anti-Evl for 30 min at room temperature and split into four batches. The supernatants were removed. Four consecutive cycles of depletion of 20 μl of brain extracts were performed at 4°C for 60 min. Mock-depleted extracts were treated identically in parallel using uncoated Dynabeads.

Profilin was depleted from platelet extracts by poly-L-proline chromatography. 50 μl of extract was chromatographed through 50-μl poly-L-proline-agarose columns that had been first equilibrated in 10 mM Tris-Cl^-, pH 7.5 buffer, then rapidly centrifuged in a bench Eppendorf centrifuge to remove interstitial buffer. The extract-loaded columns were centrifuged at 4°C for 1 min. The profilin-depleted flow-through was recovered. This operation was repeated once to obtain >98% depletion of profilin (see Marchand et al., 1995), as checked by immunoblotting. The extract thus obtained appeared to be partially depleted (~60%) in VASP. After a third chromatography step on poly-L-proline-agarose, VASP was no longer detected by immunoblotting. Since the lowest detectable amount of VASP is 20 nM and the total amount of VASP in platelet extracts is 0.7 μM (see Results), we consider that the extent of depletion of VASP was at least 97%. This last result also demonstrates that VASP binds to the poly-L-proline column.

Polymerization Measurements

VASP-induced polymerization of MgATP-G-actin was monitored at 20°C by the increase in fluorescence of pyrenyl-labeled actin using a Spex Fluorolog 2 spectrophotometer. The excitation wavelength was 366 nm, and the emission wavelength was 407 nm. The excitation and emission slits were maintained small enough so that the fluorescence measured at 407 nm was not contaminated by scattered light due to bundle formation. Alternatively, the polymerization process was monitored by turbidimetry using a Cary 1 spectrophotometer, at a wavelength of 310 nm and using 120-μl cuvettes thermostatted at 20°C. At the end of the polymerization process, samples were centrifuged at 400,000 *g* for 20 min at 20°C. The amounts of sedimented F-actin and unassembled actin were determined by SDS-PAGE of the resuspended pellets and of the supernatants. Gels were either Coomassie blue stained or silver stained according to Morrissey (1981). The gel patterns were scanned using an Arcus (Agfa) scanner and analyzed using the Image Analysis NIH software.

Electron Microscopy

Samples of preincubated MgATP-G-actin (1 μM) and VASP (1–2 μM) were deposited on air glow-discharged carbon-coated grids, negatively stained with 2% uranyl acetate, and observed in a Philips CM12 electron microscope. Electron micrographs were taken at a 35,000-fold magnification.

Results

VASP Is Required for Listeria Movement in Platelet Extracts: Role of the Interaction of the EVH1 Domain with ActA

VASP was immunodepleted from platelet extracts using magnetic Dynabeads coated with an antibody directed against the proline-rich region of VASP. *Listeria* did not move in VASP-depleted extracts, whereas the mock-depleted extracts fully supported motility as efficiently as the untreated extracts. Specifically, the fraction of motile bacteria (30–40%) was the same in the untreated and mock-depleted extracts. Although no actin tails were assembled around *Listeria* after depletion of VASP, actin actively polymerized at the surface of the bacteria into large, loosely organized, veil-like actin meshworks, as illustrated in Fig. 1. Add-back of the bacterial recombinant VASP protein at concentrations as low as 0.25 μM restored the movement of bacteria. The optimum concentration of VASP was 0.5–1 μM. Data showing the extent of VASP depletion and the dependence of the speed of bacteria on VASP concentration are displayed in Fig. 2. The speed of propulsion was not affected by addition of 1 μM VASP to the undepleted extracts. Upon addition of larger amounts of VASP (5 μM), bright actin bundles of rhodamine-F-actin were observed in platelet extracts and inhibition of movement started to be observed. Using recombinant VASP as a standard, the concentration of VASP in platelet extracts was determined to be 0.7 ± 0.2 μM by immunoblotting (Fig. 2), which corresponds to ~4 ± 1 μM in the platelet cytoplasm, assuming a sixfold dilution of the cytoplasm in the extracts (Carlier et al., 1997). The successful reconstitution

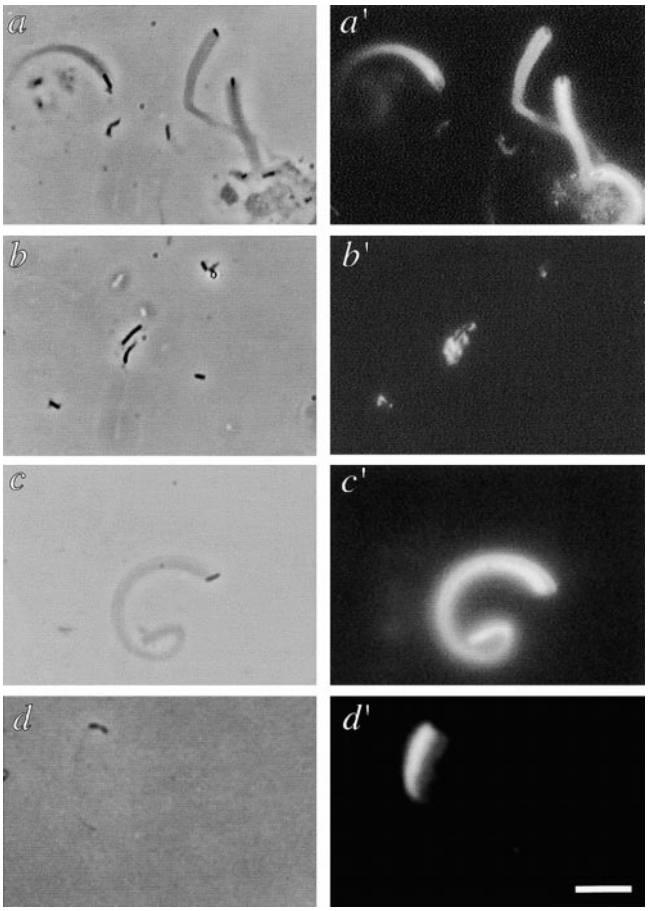

Figure 1. VASP is essential for actin-based motility of *Listeria* in platelet extracts. Actin structures formed by *L. monocytogenes* in: a and a′, mock-depleted platelet extract; b and b′, VASP-depleted extract (two cycles of depletion on anti-VASP–coated Dynabeads); c and c′, VASP-depleted extract supplemented with 1 μM bacterial recombinant VASP; d and d′, VASP-depleted extract supplemented with 0.9 μM eukaryotic recombinant VASP. (a–d) Phase-contrast; (a′–d′) corresponding rhodamine-actin fluorescence. Bar, 5 μm.

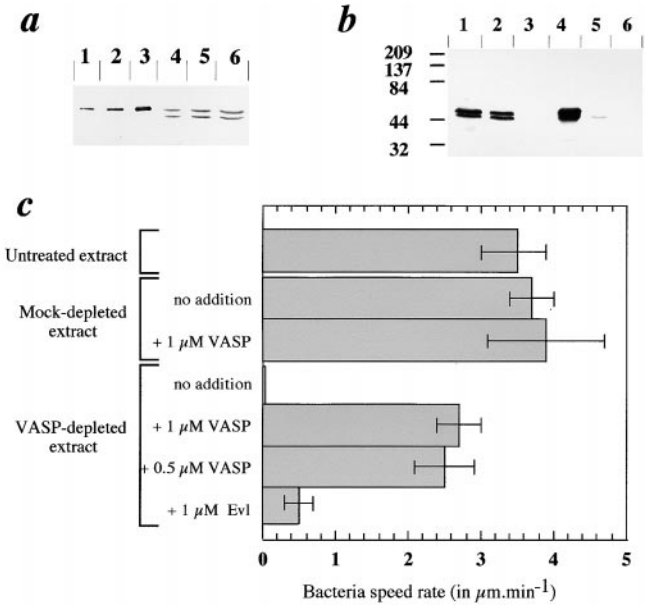

Figure 2. Immunodepletion of VASP from platelet extracts and *Listeria* movement in VASP-depleted extracts supplemented with recombinant VASP or Evl. (a) Quantitation of VASP in platelet extracts. 0.5 (lane 1), 1 (lane 2), and 2 pmol (lane 3) of recombinant VASP and 0.66 (lane 4), 1.33 (lane 5), and 2.66 μl (lane 6) of platelet extract were electrophoresed and immunoblotted using anti-VASP (M4 polyclonal antibody). Comparison of the densitometric patterns of the standards and of platelet VASP using the NIH Image analysis software led to an estimate of 0.7 μM VASP in the extracts. (b) Analysis of the immunodepletion of VASP from platelet extracts. Lane 1, whole extract; lane 2, mock-depleted extract; lane 3, VASP-depleted extract (two cycles of depletion using Dynabeads); lane 4, Dynabead-bound VASP after the first cycle of depletion; lane 5, Dynabead-bound VASP after the second cycle of depletion; and lane 6, control beads (not coated with anti-VASP) used for the mock depletion. The Western blot was revealed using M4 polyclonal anti-VASP. (c) Mean rates of movement of *Listeria* in VASP-depleted extracts and in depleted extracts supplemented with VASP or Evl recombinant proteins. 10–15 rate measurements were performed for each sample. At least three independent experiments were carried out.

of *Listeria* movement was observed with unphosphorylated bacterial VASP as well as with the eukaryotic recombinant VASP in an identical range of concentrations (Fig. 1, d and d′).

VASP has been shown to interact with ActA via its NH_2-terminal EVH1 domain. To verify the implication of this interaction in *Listeria* movement, extracts were supplemented with 2.5 μM GST-EVH1 fusion proteins of VASP, Mena, and Evl which share sequence homology (Table I). No inhibition of *Listeria* movement was observed when bacteria were added to the extracts supplemented with GST-EVH1. On the other hand, when bacteria were separately preincubated with GST-EVH1 proteins for 20 min before being added to the extracts, so that the final concentration of GST-EVH1 was again 2.5 μM, bacteria initially did not move and appeared surrounded by disorganized actin clouds. After 30 min of incubation in the extracts, bacteria slowly resumed normal movement and comet tails eventually were seen. The rate of propulsion eventually decreased at late times, most likely due to ATP depletion. These data indicate that the EVH1 domain of VASP, Mena, and Evl is in slow association–dissociation equilibrium with the poly-L-proline region of ActA. In addition, the fact that endogenous VASP at 0.7 μM eventually displaces ActA-bound EVH1 when isolated EVH1 is present at 2.5 μM indicates that the affinity of VASP in the macromolecular assembly is much higher than the affinity of EVH1 for ActA, suggesting that VASP interacts either with other regions of ActA or with partners other than ActA at the surface of *Listeria*, and these interactions strengthen its overall affinity for ActA. To discriminate between the above two possibilities, the effect of the GST-(proline-rich region of ActA) fusion protein on *Listeria* motility was tested. Addition of the fusion protein at concentrations as low as 0.8 μM (a concentration equimolar to endogenous VASP) completely blocked the movement of *Listeria*, and reduced by twofold the percentage of bacteria able to initiate assembly of actin at the bacterium surface. This result demonstrates that the proline-rich region of ActA binds VASP with high affinity, and the VASP-Pro(ActA) complex cannot further interact with ActA. Accordingly, the movement of *Listeria* was not reconstituted in VASP-depleted extracts when bacteria were preincubated with GST-EVH1 proteins.

In conclusion, VASP binds ActA via interaction of the EVH1 domain of VASP with the proline-rich region of ActA, and this interaction is necessary but not sufficient for the activity of VASP in motility. Hence the interaction of VASP with other ligands increases the overall affinity of VASP for the macromolecular assembly responsible for motility, and is necessary for actin-based motility of *Listeria*.

Overall, the sequence of the Evl protein is most similar to VASP, in particular the EVH1 domains of VASP and Evl present 61% identity. The Evl recombinant protein was found able to restore actin-based motility of *Listeria* in VASP-depleted platelet extracts (Fig. 2 c). Interestingly, the rate of movement was lower upon addition of Evl to the VASP-depleted extracts than upon addition of VASP. Since the EVH1 domains of VASP and Evl are equally able to bind ActA, this difference may be due to differences in the interaction of VASP and Evl with another partner.

Movement of Listeria in Brain Extracts: Mena and Evl Can Be Replaced by VASP

The role of Mena and Evl in *Listeria* movement was addressed using Mena knockout (−/−) animals. Mouse brain extracts prepared as described in Materials and Methods were assayed for *Listeria* movement. Images of *Listeria* undergoing actin-based motility in brain extracts are displayed in Fig. 3. The rate of propulsion was 5–10-fold slower than in platelet extracts (0.15–0.3 μm/min). Because of these very slow rates, the standard deviations in rate measurements were as high as 30–40%. For that reason, the motility data in brain extracts were not reliably expressed in terms of rates and the statistics were preferably expressed in terms of percentages of motile bacteria and of bacteria surrounded by actin "clouds" but not mov-

Table I. Movement of Listeria monocytogenes in Platelet Extracts: Role of the EVH1 Domain of Proteins of the Ena/VASP Family

Experiment	Conditions	Rate of movement	% of bacteria surrounded by actin clouds
		μm/min	
1	Control	4.5 ± 0.6 (12)	
		0 at t = 10 min	
	+ 2.5 μM GST-EVH1 (VASP)	3.9 ± 0.7 (4) at t = 30 min	
		1.6 ± 0.5 (4) at t = 120 min	
	+ 2.5 μM GST-EVH1 (Mena)	0 at t = 10 min	
	+ 2.5 μM GST-EVH1 (Evl)	0 at t = 10 min	
2	Control	5.4 ± 0.4 (11)	27 (223)
	+ 0.8 μM GST-Pro(ActA)	0	15 (324)
	+ 1.6 μM GST-Pro(ActA)	0	16 (121)

Numbers in parentheses indicate the number of measurements from which the average value was calculated. The control was performed by adding to the extract a volume of PBS equal to the volume of reagent added to the sample.

ing. In contrast to the observation made on platelet extracts, the rate of movement did not increase, but decreased, upon addition of exogenous F-actin to the motility assay mixture. Therefore, motility assays were performed without additional F-actin. Preliminary experiments showed that the percentages of motile bacteria (all motile bacteria formed comet tails) and of bacteria surrounded by actin clouds were identical in brain extracts from wild-type animals and from knockout (both heterozygous −/+ and homozygous −/−) animals, leading to the tentative conclusion that the Evl protein, homologous to Mena, is sufficient to support movement in the absence of Mena. Quantitative immunoblotting assays (Fig. 4 a) show that the 48-kD Evl protein is present at a concentration of 0.7 μM in brain extracts. Identical amounts of Evl were found in brain extracts from wild-type and Mena (−/−) animals (data not shown). Immunodepletion of Evl in wild-type or heterozygous Mena (+/−) extracts did not affect the movement of *Listeria* (Fig. 4 b). The rates of movement were the same as in the undepleted controls (within the 30% standard deviation). In contrast, partial immunodepletion of Evl in Mena (−/−) extracts (not shown) caused an appreciable inhibition of movement and of the formation of regular actin tails. A large proportion of coiled, disorganized actin comets was then seen around the bacteria. Complete inhibition of movement and a total absence of actin tails were obtained upon depletion of Evl in Mena (−/−) extracts (Fig. 4, a and c). Since the lowest detectable amount of Evl is 50 nM (see below), the extent of depletion was at least 93%. However, polymerization of actin in unorganized meshworks was still observed around the bacteria. Hence Evl, like VASP, was not required for actin polymerization per se. Add-back of 1.1 μM pure recombinant Evl to Evl-depleted extracts of Mena (−/−) mice restored *Listeria* motility. Motility was equally well restored by addition of 0.6 μM bacterial recombinant VASP. The percentage of motile bacteria in the add-back of Evl or VASP was twice lower than in the mock-depleted control. Despite this lower performance, which was less quantitatively observed in other independent experiments, the difference between the Evl-depleted samples, which are totally immotile, and the (depleted + add-back of Evl or VASP) sample was reproducible and testifies for the role of Evl or VASP in movement. In conclusion, the requirements for *Listeria* motility in Evl-depleted brain extracts of Mena (−/−) mice were identical to the ones observed in VASP-depleted platelet extracts. Addition of a twice larger amount of VASP led to the massive formation of large bundles of rhodamine-actin in the brain extract, and subsequent inhibition of the formation of actin tails.

These results show that Mena, Evl, and VASP play interchangeable roles in *Listeria* movement and most likely bind to the same molecular targets in this function.

Profilin Is Not Required for Listeria Motility, but Increases Bacterial Speed

Depletion of profilin in platelet extracts by poly-L-proline chromatography did not abolish the movement of *Listeria*. In the total absence of profilin, and 60% of endogenous VASP, obtained by two consecutive poly-L-proline chromatography steps of the platelet extracts (see Materials and Methods), *Listeria* moved at a 30% lower speed than in the mock-depleted extract. Double depletion of both VASP and profilin by three consecutive poly-L-proline affinity columns (see Materials and Methods) caused the arrest of movement. Add-back of profilin alone did not restore movement. Movement was restored in the double-depleted extracts by adding back VASP alone (60% of the bacterial speed observed in the mock-depleted extract). Further addition of profilin increased the rate of move-

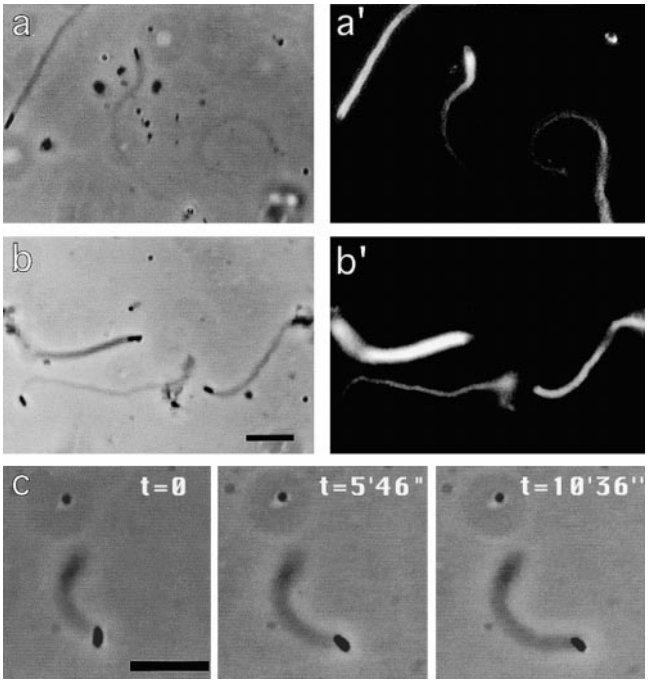

Figure 3. Movement of *L. monocytogenes* in mouse brain extracts from wild-type and Mena (−/−) animals. Typical actin tails formed in wild-type (a and a′) and in Mena (−/−) (b and b′) mouse brain extracts. (a and b) Phase-contrast; (a′ and b′) rhodamine-actin fluorescence. c shows a time-lapse illustration of the movement. Bar, 5 μm.

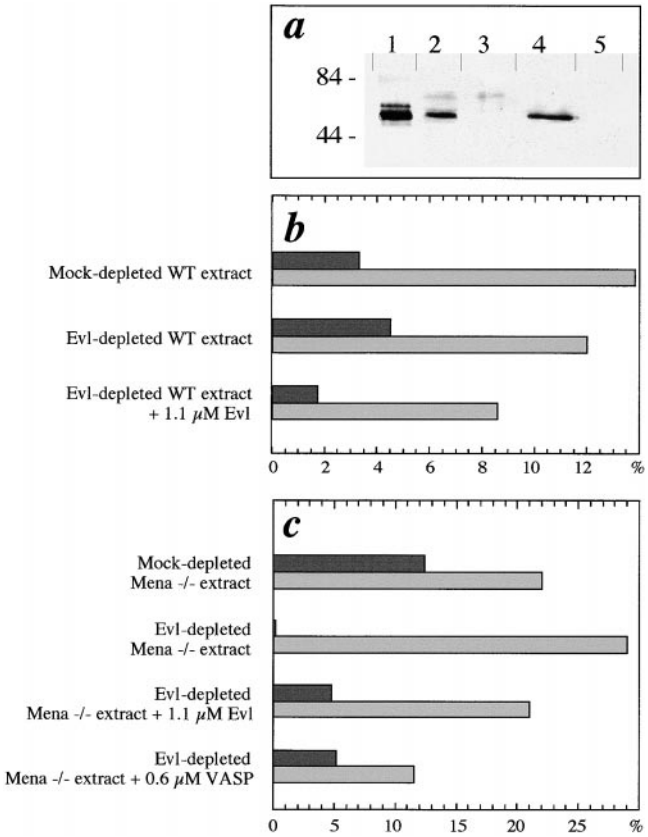

Figure 4. Evl is essential for actin-based motility of *Listeria* in mouse brain extracts. (a) Western blot analysis of Evl depletion from Mena (−/−) mouse brain extracts. Lane 1, 15 pmol of recombinant Evl; lane 2, 10 μl mock-depleted extract; lane 3, 10 μl Evl-depleted extract; lane 4, Dynabead-bound Evl after the first cycle of depletion; and lane 5, control Dynabeads used for the mock depletion. The blot was revealed using an anti-Evl mAb. (b) Effect of Evl depletion on *Listeria* movement in wild-type brain extracts. The percentages of motile bacteria, defined as: (*number of motile bacteria*/*number of total bacteria*) × 100 (dark gray bars), and of immotile bacteria that were surrounded by actin clouds, defined as: (*number of nonmotile bacteria surrounded by actin clouds*/*number of total bacteria*) × 100 (light gray bars), were determined under each condition. 271 ± 24 bacteria were counted for each measurement. Motile bacteria moved at rates that fell in the range of 0.16 ± 0.06 μm/min in all samples. (c) Effect of Evl depletion on *Listeria* movement in Mena (−/−) mouse brain extracts. Data are represented as in b. 282 ± 49 bacteria were counted for each measurement.

ment to 80% of the value observed in the mock-depleted extract (Fig. 5). These results demonstrate that profilin is not required for *Listeria* motility, in agreement with previous results obtained in *Xenopus* egg extracts (Marchand et al., 1995), and that VASP can support *Listeria* movement independent of profilin. The profilin-induced 30% increase in speed, an indication that profilin increases the efficiency of motility, may be due to profilin's known function in actin dynamics (see Discussion), or to its ability to interact directly with the (GP_5) sequence, repeated to different extents in VASP/Mena/Evl proteins. To further examine the latter possibility, the effect of the $(GP_5)_3$ peptide on *Listeria* movement in platelet extracts was assayed. Addition of the peptide at 1 mM slowed down the movement to an extent that varied widely from 20 to 60% in a large number of different experiments. The result contrasts with the very efficient inhibition of movement which was observed when micromolar amounts of this peptide were injected in infected cells (Kang et al., 1997). A similar weak and low-affinity effect was obtained upon addition of poly-L-proline (Sigma Chemical Co.) at concentrations (5–10 mM proline) comparable to those of $(GP_5)_3$. Since VASP itself binds to poly-L-proline (see Materials and Methods), we cannot eliminate the possibility that the $(GP_5)_3$ peptide and poly-L-proline inhibit movement by displacing VASP from the proline-rich region of ActA as weak competitors. The low-affinity inhibitory effect of the $(GP_5)_3$ peptide on *Listeria* movement contrasts with the very efficient inhibition observed by addition of micromolar amounts of EVH1 or Pro-ActA fusion proteins. In summary, no evidence for a functional role of the central region of VASP in *Listeria* movement can be drawn from the effect of this peptide in the present in vitro assay.

Possible Involvement of Platelet Evl and of Brain VASP in Listeria Movement

Many tissues contain two or all three proteins (Mena, VASP, Evl) of the Ena/VASP family (Lanier et al., 1999). Since these proteins play interchangeable roles in *Listeria* movement, one can legitimately wonder why the VASP present in Evl-depleted Mena (−/−) mouse brain extracts or the Evl protein present in VASP-depleted platelet extracts does not support *Listeria* movement. One possible explanation could be that the amounts of soluble Evl in platelets and of VASP in brain are so low that after depletion of the major variant (VASP in platelets, Evl in Mena (−/−) brains), the concentration of the less abundant protein is below the threshold at which movement can be observed.

To test this possibility, the amounts of Evl present in platelet extracts and of VASP in brain extracts were evaluated by quantitative immunoblotting. Fig. 6 shows that when the highest possible volumes of extracts (obtained with low ionic strength buffer, in the absence of detergent) were loaded on the gel, VASP could not be detected in brain extracts, nor Evl in platelet extracts. Considering the lower limits of immunodetection of these proteins, the result indicates that the concentration of soluble Evl in platelet extract is lower than 50 nM, and the concentration of soluble VASP in brain extracts is lower than 20 nM. These amounts appear too low to support movement of *Listeria.* Hence, our results suggest that the fraction of soluble Mena and Evl is larger than the fraction of soluble VASP in brain under the lysis conditions used to prepare these extracts. Experiments using higher ionic strength/detergent lysis indicate that pools of VASP in brain and Evl in platelets exist which are not solubilized by these conditions (Lanier et al., 1999; Gertler, F.B., unpublished observations).

VASP Interacts with Actin via Its EVH2 Domain: Implication in Listeria Movement

The above results demonstrate that VASP, Evl, and Mena play interchangeable roles in actin-based motility of *Liste-*

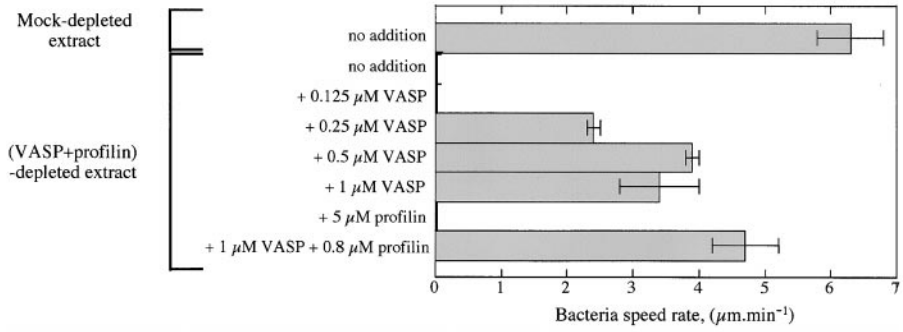

Figure 5. Profilin is not essential for actin-based motility of *Listeria* in platelet extracts. The mean rate of movement of *Listeria* was measured in mock-depleted extracts, profilin-depleted extracts, profilin + VASP double-depleted extracts, supplemented with the indicated amounts of recombinant VASP or purified bovine profilin. Mean rate values result from the average of 10 measurements.

ria. They bind ActA via their EVH1 domain and their common function implies that they interact with another unknown common ligand. Like EVH1, the EVH2 domain is well conserved among the Ena/VASP proteins. Truncation of this region abolishes the localization of VASP to focal contacts (Haffner et al., 1995), indicating that this region, like EVH1, may play a role in the targeting of VASP, though the direct contacts with ActA or zyxin are likely to be mediated only through the EVH1 domain. Since VASP appears necessary, in *Listeria* motility, to transform actin polymerization in "clouds" into an organized actin structure supporting active movement, we assayed the interaction of recombinant VASP with actin by in vitro assays combining pyrenyl-actin fluorescence, light scattering, electron microscopy, and sedimentation measurements. Such in vitro assays allow a quantitative comparison of the nonphosphorylated bacterial VASP recombinant protein with the partially phosphorylated eukaryotic recombinant VASP. Both recombinant proteins induced the polymerization of G-actin at low ionic strength, suggesting that VASP binds polymerized actin preferentially. The effect of VASP was very similar to the myosin-subfragment-1–induced assembly of G-actin (Miller et al., 1988), except that it was ATP insensitive. The polymerization process of MgATP-G-actin induced by eukaryotic recombinant VASP was monitored by the increase in fluorescence of pyrenyl-labeled actin (Fig. 7 a) and by the increase in light scattering or in turbidity at 310 nm (Fig. 7 b). Very similar, if not strictly kinetically identical data were obtained with the bacterial recombinant protein (data not shown). While the extent of pyrenyl fluorescence and the shape of the fluorescence emission spectrum were compatible with the formation of F-actin, the large increase in turbidity indicated that particles much larger than actin filaments were assembled from G-actin in the presence of VASP. The extent of fluorescence change varied with the concentration of VASP as a high-affinity titration curve (Fig. 7 a, inset), indicating that 1 mol of actin was assembled per mole of VASP monomer added, which was confirmed by sedimentation assays (not shown, but identical to data shown in Fig. 8 b). In contrast, the extent of turbidity change did not display a saturation behavior, because the thickness of the bundles increases with protein concentration and with time, resulting in a nonlinear concentration and time dependence of the turbidity. Electron microscope observation of negatively stained specimens (Fig. 7 c) showed that thick F-actin bundles were formed with bacterial and eukaryotic recombinant VASPs. The formation of bundles is fully consistent with the turbidity data. VASP-induced polymerization of G-actin was observed even at submicromolar concentrations of VASP and actin, consistent with the high affinity of VASP for F-actin at low ionic strength displayed in Fig. 7 a, inset. Polymerization was much more efficient from Mg-actin than from Ca-actin. The induction of actin assembly in filament bundles by VASP was favored in low ionic strength buffers (<20 mM KCl) and was slowed down upon increasing the ionic strength (Fig. 7 a, curves d and f; Fig. 7 b, curves d, i, and j). The formation and ionic strength dependence of F-actin bundles upon addition of VASP are both consistent with the change in charge of filaments after VASP binding and the existence of electrostatic forces between filaments in the bundles (Tang and Janmey, 1996; Tang et al., 1997). To examine

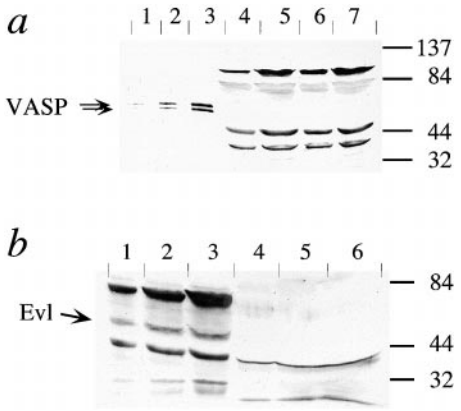

Figure 6. Immunodetection of VASP in mouse brain extracts and of Evl in platelet extracts. (a) Platelet extract (1, 2, and 4 μl, corresponding to 0.7, 1.4, and 2.1 pmol of VASP, in lanes 1, 2, and 3, respectively), Mena (−/−) mouse brain extracts (10 and 20 μl in lanes 4 and 5), and wild-type mouse brain extracts (10 and 20 μl in lanes 6 and 7) were analyzed by immunoblotting using polyclonal M4 anti-VASP antibody. Assuming that the limit of detection is 0.4 pmol, the data indicate that the maximum concentration of VASP in brain extracts is 20 nM, a concentration too low to support *Listeria* movement. (b) Wild-type mouse brain extracts (5, 10, and 20 μl corresponding to 3.5, 7, and 14 pmol of Evl in lanes 1, 2, and 3, respectively) and 10, 20, and 40 μl platelet extracts (lanes 4, 5, and 6, respectively) were analyzed by immunoblotting using a polyclonal anti-Evl antibody. Assuming that the lower limit of detection is 2 pmol Evl, the data indicate that the maximum concentration of Evl in platelets is 50 nM, which is too low to support motility of *Listeria*.

which region of VASP is involved in actin binding, the effect of the EVH2 domain, which contains the highly charged COOH-terminal region of VASP, was investigated. The GST-EVH2 fusion protein of VASP induced F-actin assembly like VASP, except that no bundles were formed (compare Fig. 7, a and b, curve g). The absence of bundles when EVH2 was bound to F-actin indicates that the overall charge of EVH2-F-actin is different from that of VASP-F-actin. Competition between VASP and GST-EVH2 was observed (Fig. 7 b, compare curves d and h).

The interaction of VASP with F-actin was then examined in vitro as follows. Preliminary sedimentation assays first showed that both bacterial and eukaryotic recombinant VASP cosedimented with F-actin (1–5 μM) in a 1:1 molar ratio of monomeric VASP per F-actin subunit, confirming the conclusions of the experiments of induction of actin assembly. The fluorescence of pyrenyl-labeled F-actin was not affected by the binding of VASP. Fig. 8 a shows that in a low ionic strength buffer (MgATP-actin, 15 mM NaCl, 0.1 mM $MgCl_2$ added to G buffer), addition of 1 μM VASP shifted the critical concentration for F-actin assembly from 0.2 to 0.1 μM, indicating that VASP increased the stability of F-actin, i.e., bound F-actin preferentially. The affinity of VASP for F-actin under physiological conditions (0.1 M KCl, 1 mM $MgCl_2$) was estimated using a sedimentation assay. The assays were performed using stan-

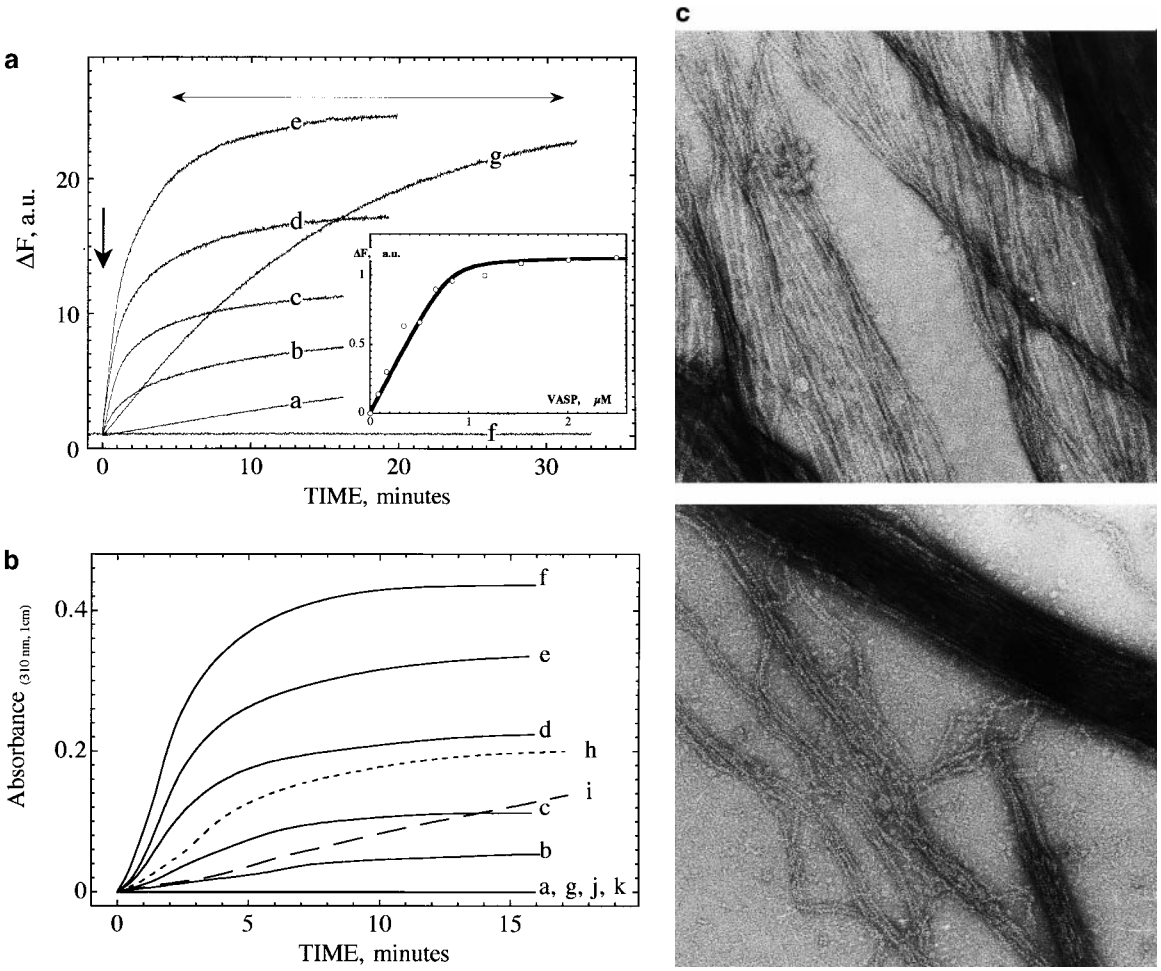

Figure 7. VASP induces polymerization of G-actin into F-actin bundles. (a) Pyrenyl-actin fluorescence measurements. 1 μM pyrenyl-labeled MgATP-G-actin was supplemented, at time indicated by the vertical arrow, with eukaryotic recombinant VASP at the following concentrations (μM): a, 0; b, 0.25; c, 0.5; d, 1; e, 2; f, 1 μM VASP + 0.1 M KCl; g, 0 VASP, 2 μM GST-EVH2. The fluorescence of 1 μM pyrenyl-G-actin is equal to 1 by convention. The horizontal arrow indicates the fluorescence measured for 1 μM F-actin polymerized in standard F buffer (0.1 M KCl, 1 mM $MgCl_2$ added to G buffer). (Inset) Extent of fluorescence change at the end of the polymerization process of 0.7 μM MgATP-G-actin induced by VASP at the indicated concentrations. Fluorescence was measured 1 h after the preparation of the samples. Final conditions were: 5 mM Tris-Cl^-, pH 7.5, 0.2 mM ATP, 0.1 mM $CaCl_2$, 1 mM DTT, 0.2 mM EGTA, 50 μM $MgCl_2$, 2 mM Hepes, 15 mM NaCl, 1% glycerol, 20°C. (b) Turbidity measurements at 310 nm. 1 μM MgATP-G-actin (same actin solution as in a) was supplemented, at time 0, with eukaryotic recombinant VASP at the following concentrations (μM): a, 0; b, 0.29; c, 0.58; d, 1.16; e, 1.74; f, 2.34; g, 0 VASP, 2 μM GST-EVH2; h, 1.16 μM VASP + 2 μM GST-EVH2; i, 1.16 μM VASP + 0.05 M KCl; j, 1.16 μM VASP + 0.1 M KCl; k, no actin, 1.16 μM VASP. Ionic conditions were as in a. Temperature was 20°C. Optical path length = 1 cm. (c) Actin bundles assembled from Mg-actin in the presence of VASP. Samples of MgATP-G-actin (1 μM) preincubated for 10 min with 1 μM VASP were negatively stained and observed in the electron microscope. (Top) Bacterial recombinant VASP. (Bottom) Eukaryotic recombinant VASP.

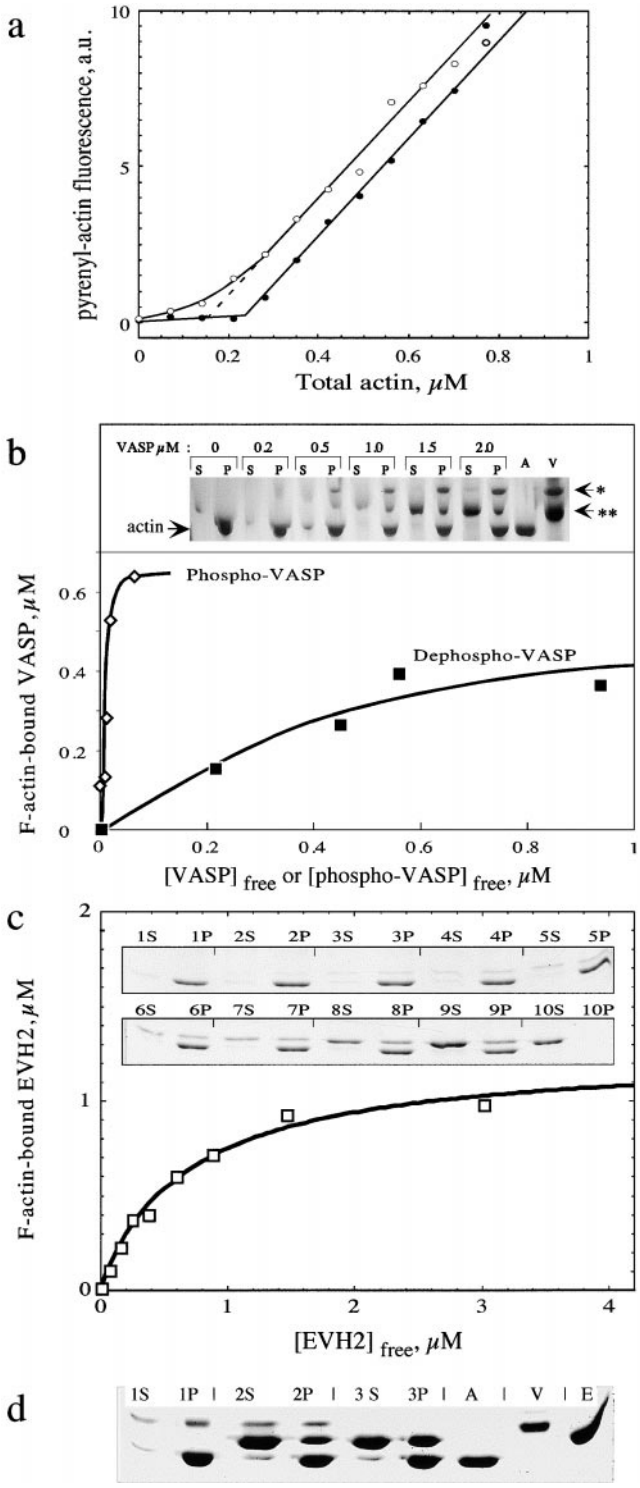

Figure 8. VASP binds to and stabilizes F-actin in a phosphorylation-regulated manner. (a) VASP shifts the critical concentration plots for actin assembly toward a lower value. Critical concentration plots for polymerization of Mg-actin in the absence (filled circles) and presence (open circles) of 1 μM eukaryotic recombinant VASP. Pyrenyl-labeled actin was polymerized at a high concentration and serially diluted in buffer adjusted to the following ionic conditions: 5 mM Tris-Cl^-, pH 7.5, 0.2 mM ATP, 0.1 mM $CaCl_2$, 0.2 mM EGTA, 0.1 mM $MgCl_2$, 1 mM DTT, 2 mM Hepes, 15 mM NaCl, and 1% glycerol. (b) Sedimentation assay for the binding of eukaryotic recombinant VASP to F-actin. Mg-F-actin was polymerized under physiological ionic conditions (0.1 M KCl, 1 mM $MgCl_2$) and mixed at 1 μM with VASP at the indicated concentrations. Samples were centrifuged for 30 min at 400,000 *g*, 20°C. Pellets were resuspended in G buffer at the original volume. Pellets (P) and supernatants (S) were submitted to SDS-PAGE. A, actin alone (1 μM); V, VASP alone (2 μM); *, 50-kD band corresponding to serine 157–phosphorylated VASP; **, 46-kD band corresponding to serine 157–unphosphorylated VASP. Data are plotted as bound VASP versus free VASP. The concentrations of free and F-actin–bound VASPs were derived from the scanning of the gels (see Materials and Methods). The curves represent the fit to the data using values of equilibrium dissociation constants K_Y = 22 nM and K_X = 0.8 μM for phospho- and dephospho-VASP, respectively (see text). (c) Sedimentation assay for EVH2 binding to F-actin. F-actin (1 μM) polymerized in physiological ionic conditions was incubated with EVH2 at the following concentrations in μM: 1, 0; 2, 0.25; 3, 0.5; 4, 0.75; 5, 1.0; 6, 1.5; 7, 2; 8, 3; 9, 5; 10, 3 μM EVH2, no actin. Supernatants (S) and pellets (P) of sedimented samples were submitted to SDS-PAGE. Data are plotted as F-actin bound EVH2 versus free EVH2 as in b. The data are analyzed as in b and the curves are fit to the data using a value of the equilibrium dissociation constant of 0.69 ± 0.1 μM. (d) Competition between GST-EVH2 and VASP for binding to F-actin. F-actin (1 μM) polymerized in physiological ionic conditions was incubated with: 1, no additions; 2, 1 μM eukaryotic recombinant VASP and 4 μM GST-EVH2; 3, 4 μM GST-EVH2. Samples were sedimented at 400,000 *g* and supernatants (S) and pellets (P) were submitted to SDS-PAGE. A, V, and E correspond to 1 μM actin, 1 μM VASP, and 4 μM GST-EVH2, respectively. Comparison of lanes 3P and 2P shows that EVH2 is displaced from F-actin by VASP.

dard F-ADP-actin and F-ADP-BeF_3-actin, which mimics the F-ADP-Pi state of F-actin, in parallel samples. The rationale for this experiment was to determine whether VASP, in being bound to ActA and to the barbed ends of growing filaments, which have F-ADP-Pi terminal subunits, would show a functionally relevant preference for either one of the F-ADP or F-ADP-Pi conformations of F-actin. No difference was observed in the binding of bacterial and eukaryotic recombinant VASPs to F-ADP and F-ADP-Pi (data not shown). On the other hand, the two eukaryotic VASP polypeptides corresponding to the serine 157–dephosphorylated form (46 kD, which we will call dephospho-VASP) and the serine 157–phosphorylated form (50 kD, which we will call phospho-VASP) bound F-actin with different affinities. Typical data displayed in Fig. 8 b show that when 0.5 μM eukaryotic VASP was mixed with 1 μM F-actin, phospho-VASP, which represented ~30% of the material, was practically all bound to F-actin, consistent with an equilibrium dissociation constant lower than 0.05 μM, while 50% of dephospho-VASP was bound to F-actin, consistent with an equilibrium dissociation constant of ~1 μM. The values of the equilibrium dissociation constants for binding of dephospho-VASP and phospho-VASP to F-actin, K_X, and K_Y, respectively, were derived from the quantitative analysis of the scanned gel patterns using a model in which the two forms of VASP bind to the same site on F-actin. The following equations were used:

$$K_X = [F]/([X_0]/[X] - 1)$$

$$K_Y = [F]/([Y_0]/[Y] - 1)$$

$$[V_0] = [X_0] + [Y_0],$$

with $[X_0] = 0.7\,[V_0]$ and $[Y_0] = 0.3\,[V_0]$. $[V_0]$, $[X_0]$, and $[Y_0]$ represent the total concentrations of VASP, of dephospho-VASP, and of phospho-VASP, respectively; $[X]$ and $[Y]$ represent the concentrations of free dephospho- and free phospho-VASP measured in the supernatants; and $[F]$ represents the concentration of unliganded F-actin subunits, derived from the difference between total F-actin and the sum of F-actin–bound phospho- and dephospho-VASP, measured in the pellets.

Values of 0.8 ± 0.1 and 0.02 ± 0.01 μM were thus found for K_X and K_Y (Fig. 8 b). In conclusion, phosphorylated VASP binds F-actin with a 40-fold higher affinity than dephosphorylated VASP.

It has been demonstrated that the shift in apparent molecular mass of VASP from 46 to 50 kD is linked to phosphorylation of serine 157 exclusively, while phosphorylation at other sites (serine 239, threonine 278) does not affect the electrophoretic migration in denaturing gels (Waldmann et al., 1987). Accordingly, both the 46-kD and the 50-kD polypeptides may be partially phosphorylated on other sites, e.g., serine 239 (Smolenski et al., 1998). Nonetheless, in its high-affinity binding to actin, the 50-kD phospho-VASP polypeptide behaves as a homogeneous population, which suggests that the phosphorylation of serine 157 is solely responsible for the strong binding to F-actin. A different, more complex, bimodal behavior would be displayed in the binding curves if phosphorylation of serine 239 affected the affinity of VASP for F-actin. In conclusion, the phosphorylation of serine 157 by the cAMP-dependent protein kinase regulates the affinity of VASP for F-actin. Our results showing that VASP binds F-actin are in qualitative agreement with earlier data using VASP purified from platelets (Reinhard et al., 1992), but the binding stoichiometry and the affinity of VASP for actin were not estimated, and the experiments were not conducted under conditions appropriate to measure a difference in affinity between phosphorylated and nonphosphorylated VASP.

Finally, cosedimentation assays, displayed in Fig. 8, c and d, showed that GST-EVH2 bound to F-actin in a 1:1 molar ratio with an equilibrium dissociation constant of 0.7 μM and in competition with VASP. In conclusion, the interaction of VASP with F-actin is mediated by its EVH2 domain.

To understand the function of the interaction of VASP with F-actin in motility of *Listeria*, the effect of the GST-EVH2 on *Listeria* movement in platelet extracts was tested. Addition of 3.5 μM GST-EVH2 to the motility assay mix led to the formation of ill-defined actin tails. Upon addition of 7 μM GST-EVH2, no actin tails were formed and bacteria did not move. These data, which corroborate the competition between VASP and EVH2 for binding to F-actin, indicate that the interaction of VASP with actin, mediated by the EVH2 domain, is essential in its function in actin-based motility. The fact that a 10-fold molar excess of EVH2 over VASP is necessary to inhibit movement, while the affinity of EVH2 and of VASP for F-actin are identical, is again consistent with the multiple interaction of VASP in the macromolecular assembly responsible for motility.

Discussion

The in vitro motility assay of *L. monocytogenes* in platelet and brain extracts has been used as a tool to demonstrate that proteins of the Ena/VASP family are required for actin-based motility. Since active actin polymerization, but no movement, is observed around the bacteria after selective removal of VASP from platelet extracts (or of Mena and Evl from brain extracts), we conclude that these proteins do not act as actual nucleators of actin assembly, but as organizers of the actin meshwork for the efficient production of propulsive force. This conclusion is in full agreement with the one derived from genetic studies showing that the deletion of the four proline-rich repeats of ActA caused a severe inhibition of *Listeria* movement in infected cells and in *Xenopus* egg extracts (Smith et al., 1996). Although bacteria expressing modified ActA still induced actin assembly, the number of bacteria moving (albeit at a fourfold reduced speed) was 10-fold lower than for wild-type bacteria. A 5.5-fold reduced speed of movement in infected cells was also observed in a second report (Niebuhr et al., 1997). The quantitative difference between the observations derived from genetically modified *Listeria* and the present in vitro VASP/Mena/Evl depletion studies lies in the fact that in the previous experiments, proteins of the Ena/VASP family were still present in the medium. Therefore, the possibility cannot be discounted that low-affinity binding of these proteins to subsites on ActA, undetectable by immunofluorescence, would be sufficient to elicit slow movement of a few bacteria. Interestingly, a motility phenotype similar to the one obtained upon VASP removal (actin polymerization around the bacteria, indicating that Arp2/3 was recruited, but no actin tail formation and no movement) was observed upon deletion of the 117-KKRRK-121 peptide in the NH_2-terminal region of ActA (Lasa et al., 1997). Although VASP was bound to these NH_2-terminal deletion ActA mutants, the phenotype suggests that it may not have been bound in a functional fashion. In summary, while the proline repeats of ActA may represent the main VASP binding subsite, other regions of ActA may also be involved in VASP function.

VASP, Mena, and Evl appear to play interchangeable roles in actin-based motility, in different cellular contexts. Evl can replace VASP in VASP-depleted platelet extracts, and VASP can replace both Mena and Evl in Mena knockout, Evl-depleted brain extracts. This conclusion is in agreement with a recent report (Ahern-Djamali et al., 1998) showing that, in vivo, human VASP can substitute for the loss of Ena in the *Drosophila* embryo. It shows that these proteins are likely to interact with the same targets in different cells, and that the role of Ena in neural development may be, in analogy with the function of VASP in *Listeria* movement, to organize the growth of filaments at the plasma membrane for the correct development of neural cells. Whether VASP, Ena, Mena, and Evl are similarly regulated in different tissues is an open question.

Ena/VASP proteins clearly can support *Listeria* movement independently of profilin, since the simple add-back of VASP to extracts that have been double-depleted from VASP and profilin is sufficient to restore movement of *Listeria* at a rate which is 75% of the rate observed upon

add-back of both VASP and profilin. *Listeria* movement does not require profilin, however the increase in bacterial speed provided by profilin is consistent with its function in filament turnover (Didry et al., 1998). In the presence of ADF (2 μM in platelet extracts), profilin increases the turnover of actin filaments, which powers the movement of *Listeria*. Whether an additional effect is provided by the interaction of VASP/Mena with profilin is an issue which is not elucidated by our work. The engineering of mutated forms of VASP unable to bind profilin but binding ActA and F-actin in an unaltered fashion, or of mutated forms of profilin unable to bind poly-L-proline but interacting with actin only, in a complex able to participate in barbed end assembly like unmodified profilin appears required to clarify this point. In this context, it is noteworthy that a recent report (Suetsugu et al., 1998) studying the role of profilin in N-WASP–elicited filopodia extension in response to EGF demonstrates that the ability of profilin to interact directly with actin is required for N-WASP–mediated filopodial extension, and that mutations in the proline-rich region of N-WASP which abolish the binding of profilin to N-WASP did not impair filopodium extension, although the length of the microspikes was greatly reduced.

The in vitro motility assay of *Listeria* provides quantitative estimates of the affinities of the different domains of the Ena/VASP proteins involved in building the molecular scaffold responsible for actin assembly and movement. The recombinant VASP and Evl proteins used in this work were efficient at submicromolar concentrations. Use of the GST-EVH1 and GST-(Pro-ActA) fusion proteins of VASP, Mena, and Evl demonstrates that the EVH1 domain itself binds the ActA proline-rich region in slow association–dissociation equilibrium, and with an affinity which, given the very slow dissociation rate, we tentatively estimate at least in the 10^7 M^{-1} range. This implies that the attachment of VASP to ActA is quasi-permanent during the movement of *Listeria*.

VASP interacts also with actin via its EVH2 domain. The isolated EVH2 domain binds F-actin in a 1:1 molar ratio and an affinity of 0.7 μM, identical to the binding stoichiometry and affinity of dephospho-VASP for F-actin. The fact that EVH2, in displacing VASP from F-actin, abolishes the movement, demonstrates that the interaction of VASP with the filaments of the actin tail is essential in propulsion. In binding its two targets, ActA and actin, VASP may work as a molecular connector linking the surface of the bacterium to the growing filament via its EVH1 and EVH2 domains. This result is in full agreement with the strong bonding between the bacterium and the actin tail measured with optical tweezers (Gerbal, F.B., V. Laurent, A. Ott, P. Chaikin, M.-F. Carlier, and J. Prost, manuscript in preparation). Our results expand the conclusion of these mechanical studies in showing that the attachment of the actin tail to the bacterium is required for movement, a conclusion at variance with the original Brownian ratchet model (Peskin et al., 1993). One can imagine that the connection elicited by VASP between ActA and actin imposes a structural constraint in the arrangement of the elongating barbed ends at the surface of *Listeria*, maintaining them attached to the bacterium and bundled in a defined orientation, which would allow the development of force in privileged location and direction. In the absence of VASP, the growing filament ends are randomly oriented, leading to the formation of disorganized actin clouds from which a productive force against the bacterium wall cannot result. The EVH2 domain of Ena has been proposed recently to be involved in multimerization of Ena (Ahern-Djamali et al., 1998). In view of the present data showing the interaction of EVH2 with actin, it is also possible that F-actin was present as a third

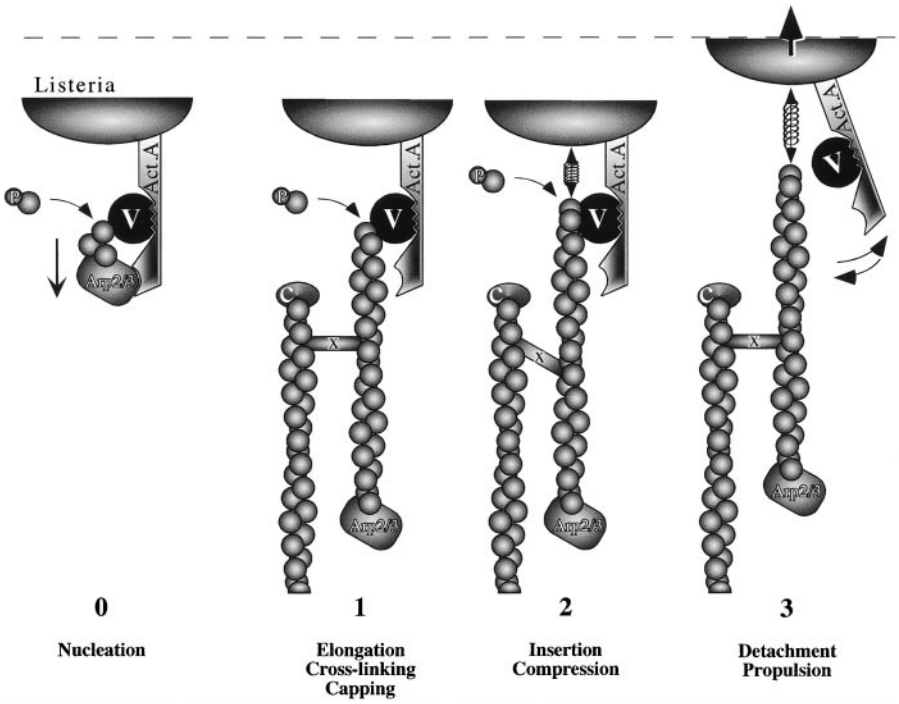

Figure 9. Working model for the role of VASP in actin-based motility. This scheme summarizes the conclusions from the present work concerning the role of VASP in *Listeria* movement. Step 0 represents nucleation of actin filaments on Arp2/3 complex in interaction with the NH_2-terminal domain of ActA. VASP (V) is bound to the central proline-rich repeats of ActA by its EVH1 domain and binds to the side of the growing filament by its EVH2 domain. Barbed end growth occurs from G-actin and from profilin (P)-actin complex. Capping of detached filaments by the capping protein (C) and cross-linking by α-actinin (x) is represented. Cycles of attachment–detachment of VASP to and from actin filaments allow insertional polymerization of actin or profilin-actin and movement as described in steps 1, 2, and 3. Insertion of subunits at the barbed end of cross-linked filaments generates compression forces used for propulsion.

partner serving to mediate or stabilize the interaction. More detailed investigations will have to be carried out to address this possibility.

The present data lead us to formulate the following model. During *Listeria* movement, VASP remains located at the bacterium–actin tail interface, implying that while the EVH1 domain is bound to ActA, the EVH2 domain slides along the side of the barbed end of the growing filament, allowing insertional polymerization of actin. This working model of a molecular ratchet is illustrated in Fig. 9. Within this model, in maintaining the site of filament growth at a defined location and distance from the bacterium surface, each added subunit would contribute in pushing the bacterium, hence VASP would increase the yield of the transformation of actin polymerization into propulsive force. Since statistically all filaments do not attach and detach simultaneously, considering the collective behavior of the population of filaments assembled at the bacterium surface is essential in understanding the mechanism of movement. Factors controlling the strength of VASP interaction with actin, i.e., the frequency of attachment–detachment steps, are expected to regulate the filament sliding rate, hence to control the speed of propulsion of *Listeria*. The fact that the affinity of VASP for F-actin is increased 40-fold (up to 0.5×10^8 M^{-1}) by phosphorylation of serine 157 raises the possibility that cAMP-dependent phosphorylation of VASP slows down the movement of *Listeria*. This possibility is currently under investigation. Our data and conclusions compare well with those derived from a recent study (Aszodi et al., 1999) showing that VASP-null platelets aggregate faster. This observation suggests that the role of VASP, which would be enhanced by phosphorylation, could be in part, via actin binding, to maintain the cohesive integrity of the membrane actin cytoskeleton of unstimulated platelets. In conclusion, the use of selectively depleted platelet and brain extracts provides a useful tool for elucidating the role of Ena/VASP family proteins in *Listeria* motility and in normal cellular function.

We thank Dominique Pantaloni for stimulating discussions. We are very grateful to Jean Lepault (Centre de Génétique Moléculaire, CNRS, Gif-sur-Yvette) for doing the electron microscopy observations of VASP-F-actin bundles shown in Fig. 7 c. We thank Dominique Didry for excellent assistance in actin purification and labeling. B.M. Jockusch and B. Harbeck thank Drs. U. Walter and Th. Jarchau (Institut für klinische Biochemie und Pathobiochemie, Würzburg, Germany) for an initial gift of VASP cDNA and S. Hüttelmaier (Braunschweig) for the GST-EVH2 vector construct used for the expression of bacterial recombinant VASP and EVH2, respectively. We wish to thank Anja Lambrechts for help with the production of recombinant Evl, and Kirsten Niebuhr for the production of the anti-Evl mAb.

This work was funded in part by the Association Francaise contre les Myopathies (AFM), the Association pour la Recherche contre le Cancer (ARC), the Ligue Nationale contre le Cancer (to M.-F. Carlier), and the Deutsche Forschungsgemeinschaft (to B.M. Jockusch). Additional funding for this research was provided by grants from Merck & Co. and by National Institutes of Health grant GM 58801-01 (to F.B. Gertler). T.P. Loisel was supported by a fellowship from the Natural Sciences and Engineering Research Council of Canada.

Received for publication 23 December 1998 and in revised form 11 January 1999.

References

Abel, K., A. Lingnau, K. Niebuhr, J. Wehland, and U. Walter. 1996. Monoclonal antibodies against the focal adhesion protein VASP revealing epitopes involved in the interaction with two VASP binding proteins and VASP phosphorylation. *Eur. J. Cell Biol.* 69(Suppl. 42):39.

Ahern-Djamali, S.M., A.R. Comer, C. Bachmann, A.S. Kastenmeier, S.K. Reddy, M.C. Beckerle, U. Walter, and F.M. Hoffmann. 1998. Mutations in *Drosophila* Enabled and rescue by human vasodilator-stimulated phosphoprotein (VASP) indicate important functional roles for Ena/VASP homology domain 1 (EVH1) and EVH2 domains. *Mol. Biol. Cell.* 9:2157–2171.

Aszodi, A., A. Pfeifer, M. Ahmad, M. Glauner, X.-H. Zhou, L. Ny, K.-E. Andersson, B. Kehrel, S. Offermans, and R. Fässler. 1999. The vasodilator-stimulated phosphoprotein (VASP) is involved in cGMP- and cAMP-mediated inhibition of agonist-induced platelet aggregation but is dispensable for smooth muscle function. *EMBO (Eur. Mol. Biol. Organ.) J.* 18:37–48.

Brindle, N.P., M.R. Holt, J.E. Davies, C.J. Price, and D.R. Critchley. 1996. The focal-adhesion vasodilator-stimulated phosphoprotein (VASP) binds to the proline-rich domain in vinculin. *Biochem. J.* 318:753–757.

Butt, E., K. Abel, M. Krieger, D. Palm, V. Hoppe, J. Hoppe, and U. Walter. 1994. cAMP- and cGMP-dependent protein kinase phosphorylation sites of the focal adhesion vasodilator-stimulated phosphoprotein (VASP) *in vitro* and in intact human platelets. *J. Biol. Chem.* 269:14509–14517.

Carlier, M.-F. 1998. Control of actin dynamics. *Curr. Opin. Cell Biol.* 10:45–51.

Carlier, M.-F., V. Laurent, J. Santolini, D. Didry, R. Melki, Y. Hong, G.-X. Xia, N.-H. Chua, and D. Pantaloni. 1997. Actin depolymerizing factor (ADF/cofilin) enhances the rate of actin filament turnover: implication in actin-based motility. *J. Cell Biol.* 136:1307–1322.

Chakraborty, T., F. Ebel, E. Domann, K. Niebuhr, B. Gerstel, S. Pistor, C.J. Temm-Grove, B.M. Jockusch, M. Reinhard, U. Walter, and J. Wehland. 1995. A focal adhesion factor directly linking intracellularly motile *Listeria monocytogenes* and *Listeria ivanovii* to the actin-based cytoskeleton of mammalian cells. *EMBO (Eur. Mol. Biol. Organ.) J.* 14:1314–1321.

Dabiri, G.A., J.M. Sanger, D.A. Portnoy, and F.S. Southwick. 1990. *Listeria monocytogenes* moves rapidly through the host cell cytoplasm by inducing directional actin assembly. *Proc. Natl. Acad. Sci. USA.* 90:11890–11894.

Didry, D., M.-F. Carlier, and D. Pantaloni. 1998. Synergy between profilin and actin depolymerization factor (ADF/cofilin) in enhancing actin filament turnover. *J. Biol. Chem.* 273:25602–25611.

Dold, F.G., J.M. Sanger, and J.W. Sanger. 1994. Intact alpha-actinin molecules are needed for both the assembly of actin into the tails and locomotion of *Listeria monocytogenes*. *Cell Motil. Cytoskeleton.* 28:97–107.

Domann, E., J. Wehland, M. Rohde, S. Pistor, M. Hartl, W. Goebel, M. Leismeister-Wächter, M. Wuenscher, and T. Chakraborty. 1992. A novel bacterial virulence gene in *Listeria monocytogenes* required for host cell microfilament interaction with homology to the proline-rich region of vinculin. *EMBO (Eur. Mol. Biol. Organ.) J.* 11:1981–1990.

Domke, T., T. Federau, K. Schluter, K. Giehl, R. Valenta, D. Schomburg, and B.M. Jockusch. 1997. Birch pollen profilin: structural organization and interaction with poly-L-proline peptides as revealed by NMR. *FEBS Lett.* 411: 291–295.

Gertler, F.B., J.S. Doctor, and F.M. Hoffmann. 1990. Genetic suppression of mutants in the *Drosophila abl* protooncogene homolog. *Science.* 248:857–860.

Gertler, F.B., A.R. Comer, J.L. Juang, S.M. Ahern, M.J. Clark, E.C. Lieb, and F.M. Hoffmann. 1995. *Enabled*: a dosage-sensitive suppressor of mutations in the *Drosophila* Abl tyrosine kinase, encodes an Abl substrate with SH3 domain binding properties. *Genes Dev.* 9:521–533.

Gertler, F.B., K. Niebuhr, M. Reinhard, J. Wehland, and P. Soriano. 1996. Mena, a relative of VASP and *Drosophila* Enabled, is implicated in the control of microfilament dynamics. *Cell.* 87:227–239.

Haffner, C., T. Jarchau, M. Reinhard, J. Hoppe, S.M. Lohmann, and U. Walter. 1995. Molecular cloning, structural analysis and functional expression of the proline-rich focal adhesion and microfilament-associated protein VASP. *EMBO (Eur. Mol. Biol. Organ.) J.* 14:19–27.

Hüttelmaier, S., O. Maybodora, B. Harbeck, T. Jarchau, B.M. Jockusch, and M. Rüdiger. 1998. The interaction of the cell-contact proteins VASP and vinculin is regulated by phosphatidylinositol-4,5-bisphosphate. *Curr. Biol.* 8:479–488.

Isambert, H., P. Venier, A.C. Maggs, A. Fattoum, R. Kassab, D. Pantaloni, and M.-F. Carlier. 1995. Flexibility of actin filaments derived from thermal fluctuations: effects of bound nucleotide, phalloidin and muscle regulatory proteins. *J. Biol. Chem.* 270:11437–11444.

Kang, F., R.O. Laine, M.R. Bubb, F.S. Southwick, and D.L. Purich. 1997. Profilin interacts with the Gly-Pro-Pro-Pro-Pro-Pro sequences of vasodilator-stimulated phosphoprotein (VASP): implications for actin-based *Listeria* motility. *Biochemistry.* 36:8384–8392.

Kocks, C., E. Gouin, M. Tabouret, P. Berche, H. Ohayon, and P. Cossart. 1992. *L. monocytogenes*-induced actin assembly requires *actA* gene product, a surface protein. *Cell.* 68:521–531.

Kouyama, T., and K. Mihashi. 1981. Fluorometry study of *N*-1-pyrenyl-iodoacetamide-labeled F-actin. *Eur. J. Biochem.* 114:33–38.

Lambrechts, A., J.L. Verschelde, V. Jonckheere, M. Goethals, J. Vandekerckhove, and C. Ampe. 1997. The mammalian profilin isoforms display complementary affinities for PIP2 and proline-rich sequences. *EMBO (Eur. Mol. Biol. Organ.) J.* 16:484–494.

Lanier, L.M., M.A. Gates, W. Witke, A.S. Menzies, A.M. Wehman, J.D. Macklis, D. Kwiatkowski, P. Soriano, and F.B. Gertler. 1999. Mena is required for neurulation and commissure formation. *Neuron.* In press.

Lasa, I., E. Gouin, M. Goethals, K. Vancompernolle, V. David, J. Vandekerck-

hove, and P. Cossart. 1997. Identification of two regions in the N-terminal domain of ActA involved in the actin comet tail formation by *Listeria monocytogenes*. *EMBO (Eur. Mol. Biol. Organ.) J.* 16:1531–1540.

Laurent, V., and M.F. Carlier. 1998. Use of platelet extracts for actin-based motility of *Listeria monocytogenes*. *In* Cell Biology: A Laboratory Handbook. Volume 2. 2nd edition. J.E. Celis, editor. Academic Press, San Diego, CA. 359–365.

MacLean-Fletcher, S., and T.D. Pollard. 1980. Identification of a factor in conventional muscle actin preparations which inhibits actin filament self-association. *Biochem. Biophys. Res. Commun.* 96:18–27.

Marchand, J.-B., P. Moreau, A. Paoletti, P. Cossart, M.-F. Carlier, and D. Pantaloni. 1995. Actin-based movement of *Listeria monocytogenes* in *Xenopus* egg extracts is due to the maintenance of uncapped barbed ends at the bacterial surface. *J. Cell Biol.* 130:331–343.

Miller, L., M. Phillips, and E. Reisler. 1988. Polymerization of G-actin by myosin subfragment-1. *J. Biol. Chem.* 263:1996–2002.

Mogilner, A., and G. Oster. 1996. Cell motility driven by actin polymerization. *Biophys. J.* 71:3030–3045.

Morrissey, J.H. 1981. Silver stain for proteins in polyacrylamide gels: a modified procedure with enhanced uniform sensitivity. *Anal. Biochem.* 117:307–310.

Mullins, R.D., J.A. Heuser, and T.D. Pollard. 1998. The interaction of Arp2/3 complex with actin: nucleation, high affinity pointed end capping, and formation of branching networks of filaments. *Proc. Natl. Acad. Sci. USA.* 95: 6181–6186.

Niebuhr, K., F. Ebel, R. Frank, M. Reinhard, E. Domann, U.D. Carl, U. Walter, F.B. Gertler, J. Wehland, and T. Chakraborty. 1997. A novel proline-rich motif present in ActA of *Listeria monocytogenes* and cytoskeletal proteins is the ligand for the EVH1 domain, a protein module present in the Ena/VASP family. *EMBO (Eur. Mol. Biol. Organ.) J.* 16:5433–5444.

O'Reilly, D.R., L.K. Miller, and V.A. Luckow. 1992. Baculovirus Expression Vectors: A Laboratory Manual. W.H. Freeman and Co., New York.

Pantaloni, D., and M.-F. Carlier. 1993. How profilin promotes actin filament assembly in the presence of thymosin β4. *Cell.* 75:1007–1014.

Peskin, C.S., G.M. Odell, and G.F. Oster. 1993. Cellular motions and thermal fluctuations: the Brownian ratchet. *Biophys. J.* 65:316–324.

Pistor, S., T. Chakraborty, U. Walter, and J. Wehland. 1995. The bacterial actin nucleator protein ActA of *Listeria monocytogenes* contains multiple binding sites for host microfilament proteins. *Curr. Biol.* 5:517–525.

Reinhard, M., M. Halbrügge, U. Scheer, C. Wiegand, B.M. Jockusch, and U. Walter. 1992. The 46/50 kD phosphoprotein VASP purified from human platelets is a novel protein associated with actin filaments and focal contacts. *EMBO (Eur. Mol. Biol. Organ.) J.* 11:2063–2070.

Reinhard, M., K. Jouvenal, D. Tripier, and U. Walter. 1995. Identification, purification and characterization of a zyxin-related protein that binds the focal adhesion and microfilament protein VASP. *Proc. Natl. Acad. Sci. USA.* 92: 7956–7960.

Reinhard, M., M. Rüdiger, B.M. Jockusch, and U. Walter. 1996. VASP interaction with vinculin: a recurring theme of interactions with proline-rich motifs. *FEBS Lett.* 399:103–107.

Rosenblatt, J., B.J. Agnew, H. Abe, J.R. Bamburg, and T.J. Mitchison. 1997. *Xenopus* actin depolymerizing factor/cofilin (XAC) is responsible for the turnover of actin filaments in *Listeria* monocytogenes tails. *J. Cell Biol.* 136: 1323–1332.

Sanger, J.M., J.W. Sanger, and F.S. Southwick. 1992. Host cell actin assembly is necessary and likely to provide the propulsive force for intracellular movement of *Listeria monocytogenes*. *Infect. Immun.* 60:3609–3619.

Sechi, A.S., J. Wehland, and J.V. Small. 1997. The isolated comet tail pseudopodium of *Listeria monocytogenes*: a tail of two actin filament populations, long and axial and short and random. *J. Cell Biol.* 137:155–167.

Smith, G.A., J.A. Theriot, and D.A. Portnoy. 1996. The tandem repeat domain in the *Listeria monocytogenes* ActA protein controls the rate of actin-based motility, the percentage of moving bacteria and the localization of vasodilator-stimulated phosphoprotein and profilin. *J. Cell Biol.* 135:647–660.

Smolenski, A., C. Bachmann, K. Reinhard, P. Hönig-Liedl, T. Jarchau, H. Hoschuetzky, and U. Walter. 1998. Analysis and regulation of vasodilator-stimulated phosphoprotein serine 239 phosphorylation *in vitro* and in intact cells using a phosphospecific monoclonal antibody. *J. Biol. Chem.* 273:20029–20035.

Spudich, J.A., and S. Watt. 1971. The regulation of rabbit skeletal muscle contraction. *J. Biol. Chem.* 246:4866–4871.

Suetsugu, S., H. Miki, and T. Takenawa. 1998. The essential role of profilin in the assembly of actin for microspike formation. *EMBO (Eur. Mol. Biol. Organ.) J.* 17:6516–6526.

Tang, J.X., and P.A. Janmey. 1996. The polyelectrolyte nature of F-actin and the mechanism of actin bundle formation. *J. Biol. Chem.* 271:8556–8563.

Tang, J.X., T. Ito, T. Tao, P. Traub, and P.A. Janmey. 1997. Opposite effects of electrostatics and steric exclusion on bundle formation by F-actin and other filamentous polyelectrolytes. *Biochemistry.* 36:12600–12607.

Theriot, J.A., T.J. Mitchison, L.G. Tilney, and D.A. Portnoy. 1992. The rate of actin-based motility of intracellular *Listeria monocytogenes* equals the rate of actin polymerization. *Nature.* 357:257–260.

Theriot, J.A., J. Rosenblatt, D.A. Portnoy, P.J. Goldschmidt-Clermont, and T.J. Mitchison. 1994. Involvement of profilin in the actin-based motility of *L. monocytogenes* in cells and cell-free extracts. *Cell.* 76:505–517.

Tilney, L.G., and D.A. Portnoy. 1989. Actin filaments and the growth, movement and spread of the intracellular bacterial parasite, *Listeria monocytogenes*. *J. Cell Biol.* 109:1597–1608.

Tilney, L.G., and M.S. Tilney. 1993. The wily ways of a parasite: induction of actin assembly by *Listeria*. *Trends Microbiol.* 1:25–31.

Tilney, L.G., P.S. Connelly, and D.A. Portnoy. 1990. Actin filament nucleation by the bacterial pathogen, *Listeria monocytogenes*. *J. Cell Biol.* 111:2979–2988.

Waldmann, R., M. Nieberding, and U. Walter. 1987. Vasodilator-stimulated protein phosphorylation in platelets is mediated by cAMP- and cGMP-dependent protein kinases. *Eur. J. Biochem.* 167:441–448.

Welch, M.D., A. Iwamatsu, and T.J. Mitchison. 1997. Actin polymerization is induced by the Arp2/3 complex at the surface of *Listeria monocytogenes*. *Nature.* 385:265–269.

Welch, M.D., J. Rosenblatt, J. Skoble, D.A. Portnoy, and T.J. Mitchison. 1998. Actin polymerization is induced by Arp2/3 protein complex at the surface of *Listeria monocytogenes*. *Science.* 281:105–108.